

# Functional Characterization of the Somatic Hypermutation Process Leading to Antibody D1.3, a High Affinity Antibody Directed Against Lysozyme

Patrick England, Roland Nageotte, Martial Renard, Anne-Laure Page, and Hugues Bedouelle<sup>1</sup>

The impact of somatic hypermutation on the affinity of Abs directed against protein Ags remains poorly understood. We chose as a model the secondary response Ab D1.3 directed against hen egg lysozyme. During the maturation process leading to this Ab, five replacement somatic mutations occurred. After reconstituting the germline Ab from which D1.3 originated, we assessed the energetic and kinetic importance of each of the somatic mutations, individually or combined, using the BIAcore apparatus. We found that the mutations induced an overall 60-fold improvement of affinity, principally due to a decrease in the kinetic rate of dissociation. We showed that their effects were additive and context independent; therefore, in the case of D1.3, the order in which somatic mutations were introduced and selected is unimportant. Interestingly, most of the affinity improvement was due to a single somatic mutation (Asn<sup>50</sup>→Tyr in V<sub>L</sub>), involving a residue that belongs to the functional interface between Ab D1.3 and lysozyme. This replacement could either establish new Van der Waals contacts between the Ab and the Ag or help stabilize the conformation of a closely situated crucial residue of the Ab paratope. The four other mutations played only a marginal part in affinity maturation; potential reasons for which these mutations were nevertheless selected are discussed. *The Journal of Immunology*, 1999, 162: 2129–2136.

Affinity maturation is an outstanding feature of the development of T cell-dependent Ab responses against antigenic challenge (1). In mammals, three different, but closely interrelated, types of phenomena lead to this maturation. First, a great diversity of Ag binding sites is generated, through V(D)J germline gene segment recombination with joining errors, followed by somatic hypermutation of the assembled variable genes. Then, the higher affinity variants are selected at the surface of B cells (2).

The molecular basis of somatic hypermutation remains largely unknown, although it has recently been shown that DNA repair following error-prone replication is involved (3). Point mutations are introduced in a stepwise manner, at an estimated rate of  $10^{-4}$ – $10^{-3}$ /base/generation ( $10^6$  times more than the spontaneous rate of mutation), with a strong bias for transitions over transversions (4). The existence of intrinsic hot spots of mutation has been revealed (5).

Somatic hypermutation occurs mainly among rapidly dividing B lymphocytes in the dark zone of the lymphoid germinal centers. Clonally related B cells, each displaying only one type of membrane Ig, then migrate into the light zone of the germinal center where they compete for Ag binding (for review, see Ref. 6). To avoid apoptosis, B cells must indeed take up Ag, which is presented in its native form at the surface of long term Ag-retaining

follicular dendritic cells (FDC)<sup>2</sup> (7). Ag-selected B cells can then give rise to bone marrow Ab-forming cells or undergo new cycles of amplification/hypermutation and selection before becoming memory lymphocytes (8).

The Ag-selected pattern of somatic mutations has been well characterized in the case of small haptenic Ags, but only for a few Abs has the functional role of these somatic mutations been assessed by site-directed mutagenesis (9–13). In these cases, it was found that only some of the somatic mutations actually improved affinity (3- to 14-fold each), while most of them had no significant effect on the affinity of the Ab for its cognate Ag.

In the case of protein Ags, much less work has been performed. For cytochrome *c*, a protein hosting a strongly immunodominant epitope, the pattern of somatic mutations could be characterized in clonally related Abs, but the functional significance of these mutations was not assessed by site-directed mutagenesis (14). In the case of an anti-idiotypic Ab, the affinity maturation process could be reconstituted and shown to be stepwise, but the different individual affinity improvements were not quantified (15).

To our knowledge, no comprehensive study of the effects of somatic mutations on the affinity of an Ab toward a protein Ag has been performed to date. Such studies are nevertheless crucial, as results obtained from anti-hapten Abs cannot be expected to extrapolate to Abs directed against protein Ags. The nature and the shape of the two types of interfaces are altogether different; in particular, Ab-protein interfaces bury a surface at least 3 times larger than Ab-hapten interfaces and statistically involve 2–3 times more contacts (16). This observation opens up the possibility that more somatically mutated residues are effectively involved in the improvement of the affinity for protein Ags than for haptens.

Protein Engineering Group (Centre National de la Recherche Scientifique-URA 1129), Unité de Biochimie Cellulaire, Institut Pasteur, Paris, France

Received for publication July 20, 1998. Accepted for publication November 4, 1998.

The costs of publication of this article were defrayed in part by the payment of page charges. This article must therefore be hereby marked *advertisement* in accordance with 18 U.S.C. Section 1734 solely to indicate this fact.

<sup>1</sup> Address correspondence and reprint requests to Dr. Hugues Bedouelle, Unité de Biochimie Cellulaire, Institut Pasteur, 28 rue du Docteur Roux, 75724 Paris Cedex 15, France. E-mail address: hbedouel@pasteur.fr

<sup>2</sup> Abbreviations used in this paper: FDC, follicular dendritic cell; HEL, hen egg lysozyme; MalE, maltose-binding protein of *Escherichia coli*; Fv, variable fragment;  $k_{on}$ , association rate constant;  $k_{off}$ , dissociation rate constant;  $K'_{d}$ , equilibrium dissociation constant;  $\Delta\Delta G$ , variation of free energy; CDR, complementarity-determining region.

Furthermore, controversy has recently arisen about the real importance of affinity maturation in the shaping of high affinity repertoires of Abs directed against protein Ags (17). First, Zinkernagel and collaborators (18) isolated early Abs directed against the vesicular stomatitis virus that were devoid of somatic mutations and nevertheless showed nanomolar avidities, without further significant improvement through somatic hypermutation. Second, no significant differences were observed between the average avidities of Abs from anti-lysozyme primary, secondary, or later responses (19).

We precisely chose as a model Ag the well-characterized monomeric protein hen egg white lysozyme (HEL). More than 100 mAbs have been raised against HEL (19–24). Cross-reaction studies using panels of evolution-related avian lysozymes have allowed identification of the general region of the Ag and some specific amino acid residues bound by each mAb. Interestingly, unlike many other protein Ags, it appears that the whole surface of HEL is potentially antigenic (19). This correlates well with the sequence data, which are available for only about 10 mAbs; none has been proven to be clonally related, although two have been shown to use a close combination of germline gene segments (25).

In this study we assessed the impact on the affinity for HEL of each replacement somatic mutation that occurred during the maturation process leading to a particular mAb. The mouse mAb D1.3 is derived from a secondary immune response (24). The genes coding for its variable domains,  $V_H$  and  $V_L$ , have been cloned and sequenced (26). The interface between the Fv fragment of D1.3 and HEL has been well characterized at both the structural (27) and the functional (28–30) level.

On the one hand, we reverted each of the somatic mutations that D1.3 contains, and on the other hand, we introduced them into the reconstituted germline antibody from which D1.3 originated.<sup>3</sup> Some mutations were introduced simultaneously to study their additivity. The kinetic parameters of the interaction between the mutant Fv fragments of D1.3 and immobilized HEL were measured using the BIAcore apparatus.

## Materials and Methods

### Identification of somatic mutations

We used both the FastA search and alignment software included in the version 9.1 of the Wisconsin Genetics Computer Group package (Madison, WI) and the DNAPLOT alignment software (developed by W. Müller and H.-H. Althaus, University of Cologne, Cologne, Germany; website: <http://www.genetik.uni-koeln.de/dnaplot/>) to compare the DNA sequences of the  $V_H$  and  $V_L$  domains of D1.3 with the sequences of the murine Ig germline gene segments that are available in the GenBank and EMBL databases.

### Mutagenesis and production of somatic mutants

Phagemid pVD91 has been previously described (31); it allows the expression of the hybrid protein  $V_H::V_L$ -MalE, in which the  $V_L$  variable domain of Ab D1.3 is covalently linked to the N-terminus of MalE and noncovalently associated with  $V_H$  to form a heterodimeric Fv fragment. We introduced mutations into the  $V_H::V_L$ -MalE hybrid by oligonucleotide site-directed mutagenesis of pVD91. The codon changes in positions H-56 (AAC→AGC), H-86 (CAC→CAG), L-50 (TAT→AAC), L-51 (ACA→GCA), and L-52 (ACA→AAA) were introduced individually or simultaneously. The mutageneses were performed as described, using the ssDNA of pVD91 or its mutant derivatives as templates (32). The sequences of the mutated genes (either  $V_H$  or  $V_L$ ) were checked by the dideoxy chain termination method, using the T7 Sequencing Kit (Pharmacia Biotech, Uppsala, Sweden). We produced and purified the native and mutant  $V_H::V_L$ -MalE hybrids and checked their full reactivity toward HEL, as previously described (30).

### Binding assays and evaluation of the kinetic data

HEL was covalently immobilized on the carboxymethylated dextran matrix of a CM5 sensor chip to a level of 500–600 resonance units, using the Amine Coupling Kit (BIAcore AB, Uppsala, Sweden). The molecular interactions between the  $V_H::V_L$ -MalE hybrids and immobilized HEL were measured with the BIAcore 2000 apparatus as previously described (30). The association and dissociation profiles were analyzed with a nonlinear least squares algorithm implemented in the BIAevaluation 2.1 software package (BIAcore AB), using double-exponential functions of time as previously described (30).

No differences in the calculated association and dissociation rates were observed in control experiments, in which reduced surface densities of immobilized HEL (down to 50 resonance units) and/or higher flow rates (up to 30  $\mu$ l/min) were used, showing that the interactions were not limited by mass transfer. Furthermore, we observed no significant difference in the kinetics of dissociation whether free HEL was present or not (at a saturating concentration of 1.5  $\mu$ M or more) as a competitive ligand for  $V_H::V_L$ -MalE, showing that no rebinding of  $V_H::V_L$ -MalE to immobilized HEL occurred during the dissociation phase with the conditions used.

## Results

### Identification of the somatic mutations in D1.3

We performed a thorough database search to identify the murine Ig germline gene segments for which the alignment with the genes coding for the variable domains of D1.3 was best. The identification was unambiguous for the mature gene coding for the  $V_L$  domain of D1.3. Indeed, the identity between the 286 5'-terminal nucleotides coding for  $V_L$ -D1.3 and the germline subgroup VK-V, isotype 12/13, variable (V) segment K2 (33) was 97.9%, compared with 74% for VK isotype 10. The identity between the 38 3'-terminal nucleotides coding for  $V_L$ -D1.3 and the germline joining (J) segment JK1 was 100%, compared with 84.2% for JK2.

For the  $V_H$  domain, there was no ambiguity concerning the V and J segments used. The identity between the 295 5'-terminal nucleotides coding for  $V_H$ -D1.3 and germline subgroup  $V_H$ -IB V-segment PJ14 (34) was 98.6%, compared with 90–91% for the next best two V segments. The identity between the 41 3'-terminal nucleotides coding for  $V_H$ -D1.3 and germline J segment JH2 was 100% compared with 83% for JH4. As for the diversity (D) region, the germline segment DSP2.10 (or DSP2.11) (35) was used in reading frame 2 (Fig. 1).

The alignment shows that three junctional errors may have occurred during the recombination of gene segments leading to the  $V_H$  mature gene, two at the V-D junction and another at the D-J junction. Subsequent somatic hypermutation appears to have resulted in 10 somatic mutations in the V segment-encoded parts of  $V_H$  and  $V_L$ , four transitions and six transversions. Five of these mutations were silent, while five others led to amino acid replacements (Table I and Fig. 2). Among these, only the residue at position 50 of  $V_L$  was in contact with the Ag in the three-dimensional structure of the Fv fragment of D1.3 liganded with HEL (27).

### Rationale for mutagenesis

In a previous study we cloned the genes coding for the Fv fragment of Ab D1.3 into a phagemid that allows its expression as a fusion with protein MalE from *Escherichia coli* (31). We have shown that the presence of MalE does not interfere with the interaction between HEL and the Fv fragment of D1.3 (30). Therefore, in this study we used Fv-MalE hybrids, in which the  $V_L$  domain is covalently linked to the N-terminus of MalE and noncovalently associated with  $V_H$ , without cleavage between the fusion partners.

We first reconstituted the germline  $V_H$  and  $V_L$  domains from which D1.3 originated, i.e., we simultaneously reverted the five nonsilent above-mentioned somatic mutations (Table I) by oligonucleotide site-directed mutagenesis. The protein that is encoded by this quintuple reversion gene is hereafter called germline Ab.

<sup>3</sup> Mutants are named with the prefix denoting the heavy chain (H) or the light chain (L) variable domain, followed by the single-letter code for the residue found in the wild-type Ab (germline or D1.3), then the sequence position, and finally the residue in the mutant.

a)

D1.3-UH PJ14	1	2	3	4	5	6	7	8	9	10	11	12	13	14	
	CAG	GTG	CAG	CTG	AAG	GAG	TCA	GGA	CCT	GGC	CTG	GTG	GCG	CCC	
	---	---	-A	---	---	---	---	---	---	---	---	---	---	---	
D1.3-UH PJ14	15	16	17	18	19	20	21	22	23	24	25	26	27	28	
	TCA	CAG	AGC	CTG	TCC	ATC	ACA	TGC	ACC	GTC	TCA	GGG	TTC	TCA	
	---	---	---	---	---	---	---	---	---	---	---	---	---	---	
D1.3-UH PJ14	29	30	31	32	33	34	35	36	37	38	39	40	41	42	
	TTA	ACC	GGC	TAT	GGT	GTA	AAC	TGG	GTT	CGC	CAG	CCT	CCA	GGA	
	---	---	---	---	---	---	---	---	---	---	---	---	---	---	
D1.3-UH PJ14	43	44	45	46	47	48	49	50	51	52	53	54	55	56	
	AAG	GGT	CTG	GAG	TGG	CTG	GGA	ATG	ATT	TGG	GGT	GAT	GGA	AAC	
	---	---	---	---	---	---	---	---	---	-A	---	---	---	-G-	
D1.3-UH PJ14	57	58	59	60	61	62	63	64	65	66	67	68	69	70	
	ACA	GAC	TAT	AAT	TCA	GCT	CTC	AAA	TCC	AGA	CTG	AGC	ATC	AGC	
	---	---	---	---	---	---	---	---	---	---	---	---	---	---	
D1.3-UH PJ14	71	72	73	74	75	76	77	78	79	80	81	82	83†	84	
	AAG	GAC	AAC	TCC	AAG	AGC	CAA	GTT	TTC	TTA	AAA	ATG	AAC	AGT	
	---	---	---	---	---	---	---	---	---	---	---	---	---	---	
D1.3-UH PJ14	85	86	87	88	89	90	91	92	93	94	95	96	97	98	
	CTG	CAC	ACT	GAT	GAC	ACA	GCC	AGG	TAC	TAC	TGT	GCC	AGA	GAG	
	---	-A	---	---	---	---	---	---	---	---	---	---	---	---	
D1.3-UH PJ14	99	100													
	AGA	G													
	-C-	-													
D1.3-UH DSP2.10 (or DSP2.11)	100	101	102	103											
	AT	TAT	AGG	C											
	-C	---	---	T											
D1.3-UH JH2	103	104	105	106	107	108	109	110	111	112	113	114	115	116	
	TT	GAC	TAC	TGG	GGC	CAA	GCC	ACC	ACT	CTC	ACA	GTC	TCC	TCA	
	---	---	---	---	---	---	---	---	---	---	---	---	---	---	

b)

D1.3-UL K2	1	2	3	4	5	6	7	8	9	10	11	12	13	14
	GAC	ATC	CAG	ATG	ACT	CAG	TCT	CCA	GCC	TCC	CTT	TCT	GCG	TCT
	---	---	---	---	---	---	---	---	---	---	---	---	---	---
D1.3-UL K2	15	16	17	18	19	20	21	22	23	24	25	26	27	28
	GTG	GGA	GAA	ACT	GTC	ACC	ATC	ACA	TGT	CGA	GCA	AGT	GGG	AAT
	---	-T	---	---	---	---	---	---	---	---	---	---	---	---
D1.3-UL K2	29	30	31	32	33	34	35	36	37	38	39	40	41	42
	ATT	CAC	AAT	TAT	TTA	GCA	TGG	TAT	CAG	CAG	AAA	CAG	GGA	AAA
	---	---	---	---	---	---	---	---	---	---	---	---	---	---
D1.3-UL K2	43	44	45	46	47	48	49	50	51	52	53	54	55	56
	TCT	CCT	CAG	CTC	CTG	GTC	TAT	TAT	ACA	ACA	ACC	TTA	GCA	GAT
	---	---	---	---	---	---	---	A-	G-	-A-	---	---	---	---
D1.3-UL K2	57	58	59	60	61	62	63	64	65	66	67	68	69	70
	GGT	GTG	CCA	TCA	AGG	TTC	AGT	GGC	AGT	GGA	TCA	GGA	ACA	CAA
	---	---	---	---	---	---	---	---	---	---	---	---	---	---
D1.3-UL K2	71	72	73	74	75	76	77	78	79	80	81	82	83	84
	TAT	TCT	CTC	AAG	ATC	AAC	AGC	CTG	CAG	CCT	GAA	GAT	TTT	GGG
	---	---	---	---	---	---	---	---	---	---	---	---	---	---
D1.3-UL K2	85	86	87	88	89	90	91	92	93	94	95	96		
	AGT	TAT	TAC	TGT	CAA	CAT	TTT	TGG	AGT	ACT	CCT	C		
	---	---	---	---	---	---	---	---	---	---	---	---		
D1.3-UL JK1	96	97	98	99	100	101	102	103	104	105	106	107	108	
	GG	ACG	TTC	GGT	GGA	GCC	ACC	AAG	CTG	GAA	ATC	AAA	CGG	
	---	---	---	---	---	---	---	---	---	---	---	---	---	

**FIGURE 1.** Comparison of the nucleotide sequences of the variable domains of D1.3 with those of the closest murine germline gene segments. A dash signifies that the nucleotide is the same in the two sequences. Somatic mutations are marked in standard characters when they are silent and in shaded characters when they lead to an amino acid replacement. Mutations due to junction errors during the V(D)J recombination are indicated in italics. *a*, Heavy chain variable domain of D1.3 (D1.3-V<sub>H</sub>) aligned with the

**Table I.** Replacements of amino acid residues during the somatic hypermutation process leading to Ab D1.3

Position	Situation	Germline Ab Residue	Ab D1.3 Residue
L-50	CDR-L2 <sup>a</sup>	Asn	Tyr <sup>b</sup>
L-51	CDR-L2	Ala	Thr
L-52	CDR-L2	Lys	Thr
H-56	CDR-H2	Ser	Asn
H-86 <sup>c</sup>	Framework	Glu	His

<sup>a</sup> According to the Chothia structure-based definition (56), the CDRs of V<sub>L</sub> include residues 26–32 (CDR-L1), 49–53 (CDR-L2), and 90–97 (CDR-L3). The CDRs of V<sub>H</sub> include residues 26–32 (CDR-H1), 52–56 (CDR-H2), and 99–104 (96–101 with the Kabat convention) (CDR-H3). The somatic mutations belong to the same regions whether the Chothia structure-based definition or the Kabat sequence-based definition of the CDRs is used.

<sup>b</sup> Only residue L-Tyr<sup>50</sup> is in contact with the Ag in the three-dimensional structure of the complex between Ab D1.3 and HEL (27).

<sup>c</sup> Residues were numbered sequentially, according to the Protein Data Bank data file convention. If the Kabat convention had been used, the numbering of the residues would be the same, except for residue H-86, which would become H-83.

We then reintroduced individually each of the five nonsilent somatic mutations (H-S56N, H-Q86H, L-N50Y, L-A51T, and L-K52T) in this germline antibody (*upper part* of Fig. 3).

To determine whether the effects of the somatic mutations were dependent on their structural context, we also reverted individually each of the five nonsilent somatic mutations in Ab D1.3 (H-N56S, H-H86Q, L-Y50N, L-T51A, and L-T52K). The resulting single reversion mutants of D1.3 were equivalent to germline Abs in which four somatic mutations (all except the reverted mutation) had occurred (*lower part* of Fig. 3).

Finally, to determine whether the effects of somatic mutations were additive, we constructed two additional derivatives of the germline Ab, one double mutant (H-S56N/Q86H) and one triple mutant (L-N50Y/A51T/K52T) (*middle part* of Fig. 3).

#### Effects of the somatic mutations on the kinetic parameters of the interaction with HEL

For each mutation, we expressed and purified the corresponding Fv-MalE hybrid, with a yield of 0.5–2 mg of pure and fully reactive protein/l of culture medium at an OD<sub>600</sub> of 1.5. No correlation between the yield and the nature of the mutation was observed (data not shown).

The  $k_{on}$ ,  $k_{off}$ , and  $K'_d$  measured at 20°C for the germline Ab, Ab D1.3, and the 12 different mutants are given in Tables II and III. Both the  $k_{on}$  and  $k_{off}$  values varied by factors of <2, at the limit of significance, except for mutation L-N50Y, its reversion counterpart L-Y50N, and the multiple mutants that included these mutations. The  $k_{off}$  and  $K'_d$  values of mutant L-N50Y were indeed 30-fold lower than those of the germline Ab (Table II), while the  $k_{off}$  and  $K'_d$  values of mutant L-Y50N were 50-fold higher than those of Ab D1.3 (Table III).

We calculated the variation in the free energy of interaction ( $\Delta\Delta G$ ) resulting from each of the five somatic mutations when introduced into the germline Ab or Abs at intermediate stages of the maturation process (Table IV). None of the mutations had

PJ14, DSP2.10, and JH2 gene segments. *b*, Light chain variable domain of D1.3 (D1.3-V<sub>L</sub>) aligned with the K2 and JK1 gene segments. †, The codon numbering used is continuous to facilitate the comparison with the crystal structure data file. The codon numbering is the same using the Kabat convention, except for codons 83, 84, and 85 of V<sub>H</sub>, which become, respectively, 82a, 82b, and 82c, and codons 86–116, which become 83–113.

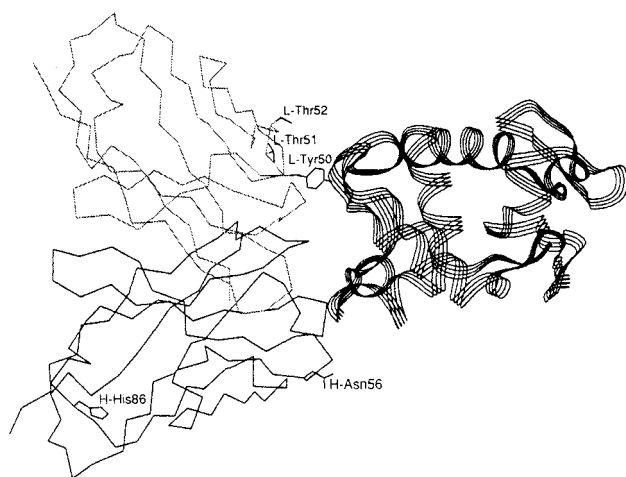


**FIGURE 2.** Structural locations of the residues of Ab D1.3 replaced during somatic hypermutation. The  $\alpha$ -carbon traces of the variable fragment of Ab D1.3 ( $V_H$ , solid lines;  $V_L$ , dashed lines) and of HEL (ribbon representation) are shown. The side chains of the mutated residues are identified by a label. The atomic coordinates were obtained from the Protein Data Bank (reference no. 1VF8).

markedly different effects according to the context in which they were introduced.

We addressed the question of the synergy between the somatic mutations by constructing some of the possible double- or triple-mutant intermediates that might have occurred during the affinity maturation process. In these cases, no significant difference between the  $\Delta\Delta G$  for the multiple mutant and the sum of the  $\Delta\Delta G$  values for the single mutants could be observed if one took into account the SEs. For instance, for the triple mutation L-N50Y/A51T/K52T,  $\Delta\Delta G(\text{L-N50Y/A51T/K52T}) = 2.08 \pm 0.13$  kcal/mol, while  $\Delta\Delta G(\text{L-N50Y}) + \Delta\Delta G(\text{L-A51T}) + \Delta\Delta G(\text{L-K52T}) = 1.87 \pm 0.15$  kcal/mol.

## Discussion

### Nature of the mutations selected during somatic maturation

By comparing the nucleotide sequences of the variable genes coding for the  $V_H$  and  $V_L$  domains of Ab D1.3 with the sequences of the germline gene segments coding for mouse Igs, which are available in various databases, we determined that 10 somatic mutations

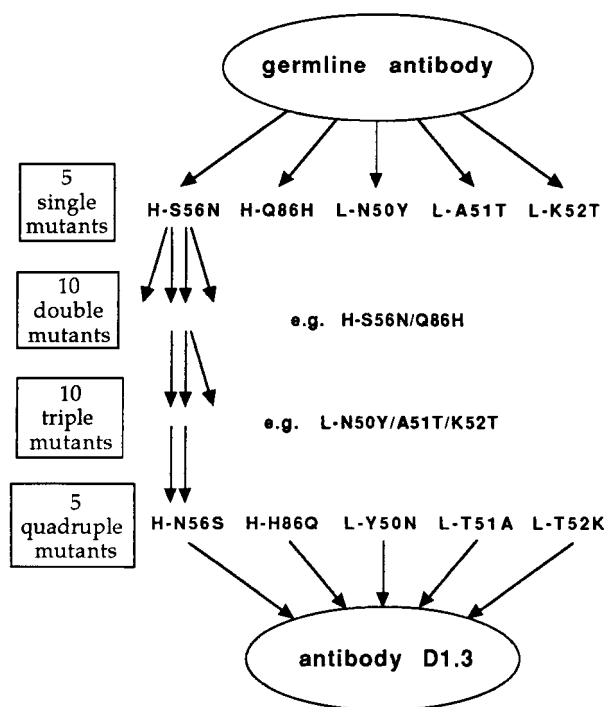


**FIGURE 3.** Schematic representation of the somatic hypermutation process and the mutagenesis strategy. Details are given in the text (see *Results*).

had occurred during the maturation process leading to D1.3. Six of the mutations were transversions, and four were transitions, even though somatic hypermutation is intrinsically biased toward transitions over transversions (4). Thus, the mutations may have been Ag selected. Furthermore, we observed that all the silent mutations were situated outside the CDRs (Fig. 1), whereas four replacement mutations of five were situated in the CDRs (Table I). The fact that a somatic replacement occurs inside a CDR has often been considered to suggest Ag selection. However, such an assertion is grossly misleading, as many CDR residues do not contribute to the energy of interaction with the Ag, while some non-CDR may play an important part. This is notably the case for Ab D1.3 (28–30, 36).

Table II. *Effects of the somatic mutations on the kinetics of interaction between the germline Ab and HEL<sup>a</sup>*

Mutation	$k_{on}$ ( $10^5 \text{ M}^{-1} \cdot \text{s}^{-1}$ )	$k_{off}$ ( $10^{-3} \text{ s}^{-1}$ )	$K'_d$ <sup>b</sup> (nM)	$\Delta G'$ (kcal $\cdot$ mol <sup>-1</sup> )
Germline Ab	$1.67 \pm 0.25$	$111 \pm 23$	$669 \pm 77$	$8.29 \pm 0.09$
H-S56N	$1.36 \pm 0.14$	$72.7 \pm 9.8$	$530 \pm 48$	$8.42 \pm 0.06$
H-Q86H	$1.41 \pm 0.15$	$73.7 \pm 8.5$	$521 \pm 42$	$8.43 \pm 0.05$
H-S56N/Q86H	$1.38 \pm 0.26$	$71.2 \pm 6.1$	$515 \pm 58$	$8.44 \pm 0.07$
L-N50Y	$1.67 \pm 0.19$	$3.78 \pm 0.36$	$23.1 \pm 3.2$	$10.25 \pm 0.08$
L-A51T	$1.78 \pm 0.21$	$111 \pm 21$	$619 \pm 88$	$8.33 \pm 0.05$
L-K52T	$1.28 \pm 0.26$	$106 \pm 17$	$835 \pm 115$	$8.16 \pm 0.08$
L-N50Y/A51T/K52T	$1.15 \pm 0.21$	$2.09 \pm 0.21$	$18.7 \pm 2.2$	$10.37 \pm 0.09$
L-A51T/K52T + H-S56N/Q86H	$1.12 \pm 0.14$	$70.8 \pm 10.5$	$628 \pm 64$	$8.32 \pm 0.06$
Ab D1.3	$1.03 \pm 0.24$	$1.15 \pm 0.09$	$11.5 \pm 1.9$	$10.64 \pm 0.08$

<sup>a</sup> The determination of  $k_{on}$ ,  $k_{off}$  and  $K'_d$  from BIAcore experimental data is described in *Materials and Methods*.  $\Delta G'$ , the free energy of dissociation from HEL, was calculated as  $-RT \ln K'_d$ , where  $R$  is the gas constant and  $T$  the absolute temperature (293 K). The mean value and associated SE of three or more independent determinations are given.

<sup>b</sup>  $K'_d$  is the equilibrium dissociation constant between Fv-MalE and HEL measured with the BIAcore apparatus at the heterogeneous interface between the liquid phase and the sensor chip. There is no simple relationship between this constant and the constant  $K_d$  that would be measured in a homogeneous solution.

Table III. *Effects of the reversion mutations on the kinetics of interaction between Ab D1.3 and HEL<sup>a</sup>*

Mutation	$k_{\text{on}}$ ( $10^5 \text{ M}^{-1} \cdot \text{s}^{-1}$ )	$k_{\text{off}}$ ( $10^{-3} \text{ s}^{-1}$ )	$K'_d$ (nM)	$\Delta G'$ (kcal $\cdot \text{mol}^{-1}$ )
Ab D1.3	1.03 ± 0.24	1.15 ± 0.09	11.5 ± 1.9	10.64 ± 0.08
H-N56S	1.04 ± 0.15	1.78 ± 0.16	17.1 ± 1.7	10.42 ± 0.06
H-H86Q	1.21 ± 0.21	1.09 ± 0.10	9.20 ± 1.26	10.78 ± 0.08
H-N56S/H86Q	1.15 ± 0.21	2.09 ± 0.21	18.7 ± 2.2	10.37 ± 0.09
L-Y50N	1.12 ± 0.14	70.8 ± 10.5	628 ± 64	8.32 ± 0.06
L-T51A	1.24 ± 0.25	2.10 ± 0.21	17.5 ± 2.7	10.41 ± 0.10
L-T52K	1.13 ± 0.13	1.30 ± 0.15	11.6 ± 1.2	10.65 ± 0.06
L-Y50N/T51A/T52K	1.38 ± 0.26	71.2 ± 6.1	515 ± 58	8.44 ± 0.07
L-T51A/T52K +H-N56S/H86Q	1.67 ± 0.19	3.78 ± 0.36	23.1 ± 3.2	10.25 ± 0.08
Germline Ab	1.67 ± 0.25	111 ± 23	669 ± 87	8.29 ± 0.09

<sup>a</sup> Legends as in Table II.

Only one of the five residues that are replaced by the hypermutation process, L-Tyr<sup>50</sup>, is actually in contact with the Ag in the crystallographic structure of the complex between the Fv fragment of Ab D1.3 and HEL (27). Structural studies of other complexes between Abs and Ags have shown that the replacement of non-contact residues by somatic hypermutation is a widespread phenomenon (37–40). However, only seldom has the functional role of distal somatic replacements been assessed and shown to be important (12, 37). No such functional characterization has yet been conducted in the case of protein Ags.

#### *Effects of the somatic mutations and structural interpretation*

We determined the kinetic parameters of the interaction between HEL and each somatic mutant using the BIAcore apparatus. First, we showed that the global affinity improvement induced by the five somatic replacements, i.e., the difference in affinity for HEL between the germline Ab and Ab D1.3, was approximately 60-fold (Table II). This result establishes clearly that for Abs directed against HEL, a significant maturation of affinity through somatic hypermutation can occur, at least in one example. The reason why the average avidity of anti-HEL Abs does not vary between the

primary and the secondary response in the study by Newman et al. (19) might be that most of the affinity maturation occurs very fast, before the early primary response Abs were isolated by day 7, or that the end-point titration assay used can only efficiently detect differences in affinity of at least an order of magnitude (as suggested by the authors themselves) and/or that the scattering of experimental points is high enough to conceal the maturation at the level of individual clones. The 60-fold improvement reported here is indeed in the upper range of affinity enhancements observed when comparing germline and hypermutated Abs directed against protein antigens (14, 15, 18, 41), whereas in the case of haptenic Ags, much higher affinity improvements through somatic hypermutation have been reported, up to 30,000-fold (40). It has been suggested that the physiological role of somatic hypermutation and selection is to allow Abs to attain a  $10^9$ – $10^{10} \text{ M}^{-1}$  avidity ceiling regardless of the starting point (17). We have shown here that the parental germline Ab of D1.3 has a micromolar affinity for the monovalent Ag HEL (Table II), and therefore the impact of affinity maturation can be important in this case. However, the affinities of other anti-HEL, and more generally anti-protein, germline Abs may be either higher or lower. In the case of highly multivalent

Table IV. *Effects of the somatic mutations on the free energy of dissociation from HEL and their dependence on the structural context*

Mutation	Context <sup>a</sup>	$\Delta\Delta G^b$ (kcal $\cdot \text{mol}^{-1}$ )
H-S56N	Germline Ab	0.13 ± 0.11
H-S56N	H-Q86H	0.01 ± 0.09
H-S56N	H-Q86H + L-N50Y/A51T/K52T	0.22 ± 0.10
H-Q86H	Germline Ab	0.14 ± 0.10
H-Q86H	H-S56N	0.02 ± 0.09
H-Q86H	H-S56N + L-N50Y/A51T/K52T	−0.14 ± 0.11
H-S56N/Q86H	Germline Ab	0.15 ± 0.11
H-S56N/Q86H	L-N50Y/A51T/K52T	0.27 ± 0.12
L-N50Y	Germline Ab	1.96 ± 0.12
L-N50Y	H-S56N/Q86H + L-A51T/K52T	2.32 ± 0.10
L-A51T	Germline Ab	0.04 ± 0.10
L-A51T	H-S56N/Q86H + L-N50Y/K52T	0.23 ± 0.13
L-K52T	Germline Ab	−0.13 ± 0.12
L-K52T	H-S56N/Q86H + L-N50Y/A51T	−0.01 ± 0.10
L-N50Y/A51T/K52T	Germline Ab	2.08 ± 0.13
L-N50Y/A51T/K52T	H-S56N/Q86H	2.20 ± 0.11
L-N50Y/A51T/K52T + H-S56N/Q86H	Germline Ab	2.35 ± 0.12

<sup>a</sup> The context is the Ab species in which the point mutation indicated in column 1 is introduced.<sup>b</sup>  $\Delta\Delta G$  values were determined as  $\Delta G'(\text{mut}2) - \Delta G'(\text{mut}1)$ , using the values of  $\Delta G'$  given in Tables II and III. mut1 represents the mutational context mentioned in column 2, and mut2 represents the additional mutation, mentioned in column 1, that was introduced in the context of column 2. For each mutation, the SE on  $\Delta\Delta G$  was calculated from the SEs on  $\Delta G'$  using the formula:  $(\text{SE}(\Delta\Delta G))^2 = (\text{SE}(\Delta G'(\text{mut}1)))^2 + (\text{SE}(\Delta G'(\text{mut}2)))^2$ .

Ags such as the vesicular stomatitis virus, some germline Abs may already attain nanomolar avidities, making further somatic hypermutation superfluous (18).

Second, we found that the affinity maturation leading to Ab D1.3 appeared to be exclusively due to a decrease in the rate of dissociation ( $k_{\text{off}}$ ) of the complex between the Ab and the Ag, which amply made up for a small decrease in the rate of association ( $k_{\text{on}}$ ). The preponderant part played by  $k_{\text{off}}$  in affinity maturation by somatic hypermutation could be a general phenomenon, as it has been observed for all the Abs that have been characterized at a kinetic level whether they were directed against protein or haptenic Ags (14, 40–42). From a theoretical standpoint, this observation could be explained by the fact that point mutations in an Ab paratope do not significantly change its overall hydrophobicity and electrostatic charge, which are preponderant for the long range attraction forces that rule  $k_{\text{on}}$ , whereas they can have a strong effect on short range interactions, such as Van der Waals or hydrogen bonds, which rule  $k_{\text{off}}$  (30). This interpretation is backed by the fact that, unlike point mutations, the global CDR replacements that occur upon repertoire shift lead principally to improvements in  $k_{\text{on}}$  (42).

The main and most unexpected feature of the affinity maturation process leading to Ab D1.3 was that it appeared to be driven almost exclusively by one somatic mutation, L-N50Y. The 30-fold decreases in  $k_{\text{off}}$  and  $K'_d$  that it induced, are the highest reported to date for a single somatic mutation in any Ab. Indeed, the 9000-fold increase in affinity that has been reported in one case does not correspond to a replacement due to somatic hypermutation, but to a joining error during the V(D)J recombination of germline gene segments (43). Abs that are directed against small haptens and for which only one or few somatic mutations play a preponderant part in affinity maturation have often been observed (9–12). However, it had been hypothesized that affinity maturation of Abs directed against protein Ags would involve a large number of small affinity improvements (15). Our results clearly refute this theory and show that the hapten paradigm can also be applied to Abs directed against protein Ags, at least in the case of Ab D1.3.

The importance of somatic mutation L-N50Y can be better understood by analyzing the functional effects of other mutations at this position and the contacts that residue L-Tyr<sup>50</sup> establishes in the crystal structure of the complex between HEL and the Fv fragment of Ab D1.3 (27, 28, 30). Mutation L-Y50F had previously been constructed in Ab D1.3 and shown to induce only a 2- to 4-fold increase in  $k_{\text{off}}$  and  $K'_d$  (28, 30). These data suggest that the main effect of L-N50Y is not the establishment of contacts between the O<sup>n</sup>H group of L-Tyr<sup>50</sup> and HEL, either directly or mediated by water molecules (27). The appearance of an aromatic cycle at position 50 could be the key feature of L-N50Y: tyrosine would have been selected because one of its corresponding codons (TAT) could be reached through a single mutation from the original asparagine codon (AAT) used in the germline V-K2 gene segment, unlike those for phenylalanine or tryptophan. The observation of the crystal structure can help explain the importance of an aromatic cycle in position L-50. On the one hand, the aromatic cycle of L-Tyr<sup>50</sup> and the side chains of two residues of HEL (Asp<sup>18</sup> and Asn<sup>19</sup>) form Van der Waals contacts, which could be energetically important. On the other hand, the aromatic cycles of L-Tyr<sup>50</sup> and L-Tyr<sup>32</sup> are parallel and closely in contact in the crystal structure; this geometry is favorable for aromatic stacking, and L-Tyr<sup>50</sup> could stabilize the side chain of L-Tyr<sup>32</sup> in an optimal configuration for the establishment of hydrogen bonds with HEL. The correct positioning of the O<sup>n</sup> atom of L-Tyr<sup>32</sup> is indeed crucial, as shown by mutation L-Y32F, which induces a 30- to 40-fold increase in  $k_{\text{off}}$  and  $K'_d$  (28, 30).

The contrast between the importance of mutation L-N50Y and the apparent needlessness of the other four somatic replacements in terms of affinity maturation was striking; indeed, mutations L-A51T and L-K52T had no detectable effect, while H-S56N and H-Q86H induced hardly significant decreases in  $k_{\text{off}}$  and  $K'_d$  (Table II). We contemplated the possibility that these mutations, although unimportant individually, played a synergistic part in affinity maturation. In this case, the  $\Delta\Delta G$  induced by a multiple somatic replacement ( $\Delta\Delta G_{\text{multiple}}$ ) would be higher than the sum of the  $\Delta\Delta G$  values induced by its constituent single mutations ( $\Sigma(\Delta\Delta G_{\text{single}})$ ). However, we observed neither long range synergy between mutations H-S56N and H-Q86H ( $\Delta\Delta G_{\text{multiple}} = 0.15 \pm 0.11$  kcal/mol;  $\Sigma(\Delta\Delta G_{\text{single}}) = 0.27 \pm 0.12$  kcal/mol) nor close range synergy between mutations L-Y50N, L-A51T, and L-K52T ( $\Delta\Delta G_{\text{multiple}} = 2.08 \pm 0.13$  kcal/mol;  $\Sigma(\Delta\Delta G_{\text{single}}) = 1.87 \pm 0.15$  kcal/mol). This suggested that the individual effects of the somatic mutations were independent and additive, and in particular that mutations L-A51T and L-K52T had no close range indirect effects on the residue in position L-50, whose importance has been discussed above.

To further investigate potential synergies between the somatic mutations, we reverted each of them, alone or in combination, in Ab D1.3. In this configuration, mutations H-H86Q and L-T52K had no detectable effect, while H-N56S and L-T51A induced hardly significant increases in  $k_{\text{off}}$  and  $K'_d$ , and multiple reversion mutations did not display any synergistic effect (Table III). Our results also showed that the somatic mutations induced the same  $\Delta\Delta G$ , taking into account the SEs, when introduced into the germline antibody or reverted in Ab D1.3, alone or in combination (Table IV). The effect of the somatic mutations on affinity was therefore context independent, suggesting that during the in vivo process of somatic maturation that led to Ab D1.3, the order in which mutations occurred and were selected was unimportant. This conclusion cannot be extrapolated to other Abs, especially if their affinity maturation relies on several key mutations, instead of one as for Ab D1.3. Indeed, in each of the two other cases where the affinity maturation by hypermutation has been characterized to the same extent of thoroughness as here (i.e., for two Abs directed against haptens *p*-azophenylarsionate and phosphocholine), three key mutations drive the affinity maturation process and the effects of the somatic mutations are context dependent and nonadditive (12, 13, 38).

#### *Hypotheses about the potential role of neutral somatic mutations*

As discussed above, the reason why somatic mutations L-A51T, L-K52T, H-S56N, and H-Q86H were selected remains unclear. One possibility is that the small improvements in affinity induced by the mutations L-A51T, H-S56N, and H-Q86H are significant at some stage of the selection process. It is unlikely that these marginal improvements grant any selective advantage to an Ab during the competition for Ag capture from the FDC, but small differences in affinity may lead to profound changes in further steps, such as the processing and presentation of Ag to the T lymphocytes (44, 45).

Another possibility is that somatic mutations L-A51T, L-K52T, H-S56N, and H-Q86H are truly neutral in terms of affinity maturation. In this case, three different types of explanations could be given for the presence of these mutations.

1) Some of the neutral mutations might have been coselected together with mutation L-N50Y or may reflect a background of mutational noise. At present, the frequency at which the Ab-bearing B lymphocytes are confronted to the Ag-bearing FDC is unknown. Theoretical calculations have suggested that hypermutation could generate as many as three somatic mutations before the

Abs face selection in the presence of Ag (46). Although these predictions await experimental confirmation, they could explain the existence of at least some of the four neutral somatic mutations in Ab D1.3. It has also been shown that high doses of injected immunogens, such as those given to the mice that produced Ab D1.3, favor a strong background of neutral somatic mutational noise (47).

2) Some mutations may reflect intrinsic mutational hot spots of the somatic hypermutation machinery. H-S56N is the only mutation, in the case of Ab D1.3, that could be due to the presence of a characterized hot spot of hypermutation; indeed, the original germline codon for H-Ser<sup>56</sup> (AGC) is in the context of the well-established (A/G)G(C/T)(A/T) hot spot motif (AGCA in this case; Fig. 1) (5).

3) The neutral mutations may grant a selective advantage according to criteria other than affinity. For example, it has been shown that mutations in V genes may affect the folding of Abs (48), their secretion (49, 50), their glycosylation (51), or their physical stability (52, 53). The analysis of the crystallographic structure of the Fv fragment of Ab D1.3 shows that the side chain of residue L-Thr<sup>51</sup> is totally buried inside the molecule, while those of residues L-Thr<sup>52</sup>, H-His<sup>86</sup>, and H-Asn<sup>56</sup> are largely accessible to the solvent. Somatic mutation L-A51T could establish new contacts between the side chain of L-Thr<sup>51</sup> and the backbone and/or the side chains of residues L-Asn<sup>31</sup>, L-Ser<sup>65</sup>, L-Gly<sup>66</sup>, and L-Tyr<sup>71</sup>, and therefore stabilize the  $\beta$ -pleated structure of V<sub>L</sub>. Other important factors might be the level of intracellular expression, the solubility, the interaction with folding chaperones, and the susceptibility toward proteolytic degradation. The maturation process may also affect the relative stabilities of the different conformational isomers of the same Ab, leading to a more favorable isomeric equilibrium (54). Moreover, Ag-driven selection operates on membrane-bound Igs, and somatic mutations may affect their interaction with other membrane constituents.

Most likely, a combination of the three points discussed above is involved in the selection of mutations L-A51T, L-K52T, H-S56N, and H-Q86H. To test whether these neutral mutations are significant and whether the importance of mutation L-N50Y leads to its recurrent selection, and to identify whether other patterns of somatic mutations could result in efficient affinity maturation, it would be interesting to isolate, in HEL-immunized mice, other mAbs that would use exactly the same V(D)J germline gene segment combination as Ab D1.3. Until now, no such mAb has been identified, although partial N-terminal peptide sequencing suggests that mAb HyHEL7 may use the same V<sub>H</sub> and V<sub>K</sub> gene segments as D1.3 (25). However, the D and J segments used may not be the same, as HyHEL7 does not appear to recognize the same HEL epitope as D1.3 (19). Another possibility would be, taking as a starting point the germline Ab from which D1.3 originated, to perform artificial affinity maturation experiments using in vitro or in vivo random mutagenesis protocols combined with selection by phage display (28, 55). We are currently conducting such experiments.

## References

- Siskind, G. W., and B. Benacerraf. 1969. Cell selection by antigen in the immune response. *Adv. Immunol.* 10:1.
- Rajewsky, K. 1996. Clonal selection and learning in the antibody system. *Nature* 381:751.
- Cascalho, M., J. Wong, C. Steinberg, and M. Wabl. 1998. Mismatch repair co-opted by hypermutation. *Science* 279:1207.
- Neuberger, M. S., and C. Milstein. 1995. Somatic hypermutation. *Curr. Opin. Immunol.* 7:248.
- Rogozin, I. B., and N. A. Kolchanov. 1992. Somatic hypermutagenesis in immunoglobulin genes. II. Influence of neighbouring base sequences on mutagenesis. *Biochim. Biophys. Acta* 1171:11.
- Han, S., B. Zheng, Y. Takahashi, and G. Kelsoe. 1997. Distinctive characteristics of germinal center B cells. *Semin. Immunol.* 9:255.
- Schriever, F., and L. M. Nadler. 1992. The central role of follicular dendritic cells in lymphoid tissues. *Adv. Immunol.* 51:243.
- Smith, K. G. C., A. Light, G. J. V. Nossal, and D. M. Tarlinton. 1997. The extent of affinity maturation differs between the memory and antibody-forming cell compartments in the primary immune response. *EMBO J.* 16:2996.
- Berek, C., and C. Milstein. 1987. Mutation drift and repertoire shift in the maturation of the immune response. *Immunol. Rev.* 96:23.
- Allen, D., T. Simon, F. Sablitzky, K. Rajewsky, and A. Cumano. 1988. Antibody engineering for the analysis of affinity maturation of an anti-hapten response. *EMBO J.* 7:1995.
- Sharon, J., M. L. Gefter, L. J. Wysocki, and M. N. Margolies. 1989. Recurrent somatic mutations in mouse antibodies to *p*-azophenylarsenate increase affinity for hapten. *J. Immunol.* 142:596.
- Sharon, J. 1990. Structural correlates of high antibody affinity: three engineered amino acid substitutions can increase the affinity of an anti-*p*-azophenylarsenate antibody 200-fold. *Proc. Natl. Acad. Sci. USA* 87:4814.
- Brown, M., M. Stenzel-Poore, S. Stevens, S. K. Kondoleon, J. Ng, H. P. Bächinger, and M. B. Rittenberg. 1992. Immunologic memory to phosphocholine keyhole limpet hemocyanin: recurrent mutations in the  $\lambda$ 1 light chain increase affinity for antigen. *J. Immunol.* 148:339.
- Mueller, C. M., and R. Jemmerson. 1996. Maturation of the antibody response to the major epitope on the self antigen mouse cytochrome *c*: restricted V gene usage, selected mutations and increased affinity. *J. Immunol.* 157:5329.
- Kocks, C., and K. Rajewsky. 1988. Stepwise intraclonal maturation of antibody affinity through somatic hypermutation. *Proc. Natl. Acad. Sci. USA* 85:8206.
- Webster, D. M., A. H. Henry, and A. R. Rees. 1994. Antibody-antigen interactions. *Curr. Opin. Struct. Biol.* 4:123.
- Foote, J., and H. N. Eisen. 1995. Kinetic and affinity limits on antibodies produced during immune responses. *Proc. Natl. Acad. Sci. USA* 92:1254.
- Kalinke, U., E. M. Bucher, B. Ernst, A. Oxenius, H.-P. Roost, S. Geley, R. Kofler, R. M. Zinkernagel, and H. Hengartner. 1996. The role of somatic mutation in the generation of the protective humoral immune response against vesicular stomatitis virus. *Immunity* 5:639.
- Newman, M. A., C. R. Mainhart, C. P. Mallett, T. B. Lavoie, and S. J. Smith-Gill. 1992. Patterns of antibody specificity during the BALB/c immune response to hen eggwhite lysozyme. *J. Immunol.* 149:3260.
- Kobayashi, T., H. Fujio, K. Hondo, Y. Dohi, A. Hirayama, Y. Takagaki, G. Kosaki, and T. Amano. 1982. A monoclonal antibody specific for a distinct region of hen egg-white lysozyme. *Mol. Immunol.* 19:619.
- Smith-Gill, S. J., A. C. Wilson, M. Potter, R. J. Feldmann, and C. R. Mainhart. 1982. Mapping the antigenic epitope for a monoclonal antibody against avian lysozyme. *J. Immunol.* 128:314.
- Smith-Gill, S. J., T. B. Lavoie, and C. R. Mainhart. 1984. Antigenic regions defined by monoclonal antibodies correspond to structural domains of avian lysozyme. *J. Immunol.* 133:384.
- Metzger, D. W., L.-K. Ch'ng, A. Miller, and E. E. Sercarz. 1984. The expressed lysozyme-specific B cell repertoire. I. Heterogeneity in the monoclonal anti-hen egg white lysozyme specificity repertoire, and its difference from the in situ repertoire. *Eur. J. Immunol.* 14:87.
- Harper, M., F. Lema, G. Boulot, and R. J. Poljak. 1987. Antigen specificity and cross-reactivity of monoclonal anti-lysozyme antibodies. *Mol. Immunol.* 24:97.
- Smith-Gill, S. J., C. R. Mainhart, T. B. Lavoie, S. Rudikoff, and M. Potter. 1984. V<sub>L</sub>-V<sub>H</sub> expression by monoclonal antibodies recognizing avian lysozyme. *J. Immunol.* 132:963.
- Ward, E. S., D. Güssow, A. D. Griffiths, P. T. Jones, and G. Winter. 1989. Binding activities of a repertoire of single immunoglobulin variable domains secreted from *Escherichia coli*. *Nature* 341:544.
- Bhat, T. N., G. A. Bentley, G. Boulot, M. I. Greene, D. Tello, W. Dall'Acqua, H. Souchon, F. P. Schwarz, R. A. Mariuzza, and R. J. Poljak. 1994. Bound water molecules and conformational stabilization help mediate an antigen-antibody association. *Proc. Natl. Acad. Sci. USA* 91:1089.
- Hawkins, R. E., S. J. Russell, M. Baier, and G. Winter. 1993. The contribution of contact and non-contact residues of antibody in the affinity of binding to antigen: the interaction of mutant D1.3 antibodies with lysozyme. *J. Mol. Biol.* 234:958.
- Dall'Acqua, W., E. R. Goldman, E. Eisenstein, and R. A. Mariuzza. 1996. A mutational analysis of the binding of two different proteins to the same antibody. *Biochemistry* 35:9667.
- England, P., F. Brégégère, and H. Bedouelle. 1997. Energetic and kinetic contributions of contact residues of antibody D1.3 in the interaction with lysozyme. *Biochemistry* 36:164.
- Brégégère, F., J. Schwartz, and H. Bedouelle. 1994. Bifunctional hybrids between the variable domains of an immunoglobulin and the maltose-binding protein of *Escherichia coli*: production, purification and antigen binding. *Protein Engin.* 7:271.
- Kunkel, T. A., J. D. Roberts, and R. A. Zakour. 1987. Rapid and efficient site-specific mutagenesis without phenotypic selection. *Methods Enzymol.* 154:367.
- Nishioka, Y., and P. Leder. 1980. Organization and complete sequence of identical embryonic and plasmacytoma  $\kappa$  V-region genes. *J. Biol. Chem.* 255:3691.
- Sakano, H., R. Maki, Y. Kurosawa, W. Roeder, and S. Tonegawa. 1980. Two types of somatic recombination are necessary for the generation of complete immunoglobulin heavy-chain genes. *Nature* 286:676.
- Decker, D. J., N. E. Boyle, J. A. Koziol, and N. R. Klinman. 1991. The expression of the Ig H chain repertoire in developing bone marrow B lineage cells. *J. Immunol.* 146:350.

36. Foote, J., and G. Winter. 1992. Antibody framework residues affecting the conformation of the hypervariable loops. *J. Mol. Biol.* 224:487.
37. Chien, N. C., V. A. Roberts, A. M. Giusti, M. D. Scharff, and E. D. Getzoff. 1989. Significant structural and functional change of an antigen-binding site by a distant amino acid substitution: proposal of a structural mechanism. *Proc. Natl. Acad. Sci. USA* 86:5532.
38. Strong, R. K., G. A. Petsko, J. Sharon, and M. N. Margolies. 1991. Three-dimensional structure of murine anti-*p*-azophenylarsonate Fab 36–71.1: x-ray crystallography, site-directed mutagenesis, and modeling of the complex with hapten. *Biochemistry* 30:3739.
39. Spinelli, S., and P. M. Alzari. 1994. Structural implications of somatic mutations during the immune response to 2-phenylloxazolone. *Res. Immunol.* 145:41.
40. Patten, P. A., N. S. Gray, P. L. Yang, C. B. Marks, G. J. Wedemayer, J. J. Boniface, R. C. Stevens, and P. G. Schultz. 1996. The immunological evolution of catalysis. *Science* 271:1086.
41. Karlsson, R., J. A. Mo, and R. Holmdahl. 1995. Binding of autoreactive mouse anti-type II collagen antibodies derived from the primary and the secondary immune response investigated with the biosensor technique. *J. Immunol. Methods* 188:63.
42. Foote, J., and C. Milstein. 1991. Kinetic maturation of an immune response. *Nature* 352:530.
43. Lavoie, T. B., W. N. Drohan, and S. J. Smith-Gill. 1992. Experimental analysis by site-directed mutagenesis of somatic mutation effects on affinity and fine specificity in antibodies specific for lysozyme. *J. Immunol.* 148:503.
44. Aluvihare, V. R., A. A. Khamlichi, G. T. Williams, L. Adorini, and M. S. Neuberger. 1997. Acceleration of intracellular targeting of antigen by the B-cell antigen receptor: importance depends on the nature of the antigen-antibody interaction. *EMBO J.* 16:3553.
45. Guernonprez, P., P. England, H. Bedouelle, and C. Leclerc. 1998. The rate of dissociation between antibody and antigen determines the efficiency of antibody-mediated antigen presentation to T cells. *J. Immunol.* 161:4542.
46. Oprea, M., and A. S. Perelson. 1997. Somatic mutation leads to efficient affinity maturation when centrocytes recycle back to centroblasts. *J. Immunol.* 158:5155.
47. Gonzalez-Fernandez, A., and C. Milstein. 1998. Low antigen dose favours selection of somatic mutants with hallmarks of antibody affinity maturation. *Immunology* 93:149.
48. Knappik, A., and A. Plückthun. 1995. Engineered turns of a recombinant antibody improve its in vivo folding. *Protein Engin.* 8:81.
49. Chen, C., T. M. Martin, S. Stevens, and M. B. Rittenberg. 1994. Defective secretion of an immunoglobulin caused by mutations in the heavy chain complementarity determining region 2. *J. Exp. Med.* 180:577.
50. Wiens, G. D., K. A. Heldwein, M. P. Stenzel-Poore, and M. B. Rittenberg. 1997. Somatic mutation in V<sub>H</sub> complementarity-determining region 2 and framework region 2: differential effects on antigen binding and Ig secretion. *J. Immunol.* 159:1293.
51. Wallick, S. C., E. A. Kabat, and S. L. Morrison. 1988. Glycosylation of a V<sub>H</sub> residue of a monoclonal antibody against  $\alpha(1-6)$  dextran increases its affinity for antigen. *J. Exp. Med.* 168:1099.
52. Hurler, M. R., L. R. Helms, L. Li, W. Chan, and R. Wetzel. 1994. A role for destabilizing amino acid replacements in light-chain amyloidosis. *Proc. Natl. Acad. Sci. USA* 91:5446.
53. Steipe, B., B. Schiller, A. Plückthun, and S. Steinbacher. 1994. Sequence statistics reliably predict stabilizing mutations in a protein domain. *J. Mol. Biol.* 240:188.
54. Foote, J., and C. Milstein. 1994. Conformational isomerism and the diversity of antibodies. *Proc. Natl. Acad. Sci. USA* 91:10370.
55. Low, N. M., P. Holliger, and G. Winter. 1996. Mimicking somatic hypermutation: affinity maturation of antibodies displayed on bacteriophage using a mutator strain. *J. Mol. Biol.* 250:359.
56. Chothia, C., A. M. Lesk, A. Tramontano, M. Levitt, S. J. Smith-Gill, G. Air, S. Sheriff, E. A. Padlan, D. Davies, W. R. Tulip, et al. 1989. Conformations of immunoglobulin hypervariable regions. *Nature* 342:877.